A Periodic Density Functional Theory Analysis of the Effect of Water Molecules on Deprotonation of Acetic Acid over Pd(111)

Sanket K. Desai, Venkataraman Pallassana, and Matthew Neurock*

Department of Chemical Engineering, University of Virginia, Charlottesville, Virginia 22903

Received: August 2, 2000; In Final Form: April 13, 2001

Nonlocal gradient corrected periodic density functional theory (DFT) was used to investigate the effect of water on the dissociation of acetic acid to the acetate anion and its corresponding proton on the Pd(111) surface. In the gas phase, the homolytic dissociation of acetic acid into acetate and hydrogen radicals (+468 kJ/mol) is clearly favored over its heterolytic dissociation into the acetate anion and proton (+1483 kJ/mol). In the presence of water, however, the heterolytic dissociation of acetic acid was found to be thermoneutral. The charged products (acetate ion and proton) are strongly stabilized by water. The metal surface acts to lower the endothermicity of the dissociation step. The energy of dissociation of acetic acid over Pd(111) was found to be +28 kJ/mol in the vapor phase. An analysis of the charge indicates that the dissociation of acetic acid over Pd(111) in the vapor phase is homolytic, forming products which are free radical like. The dissociation of acetic acid over Pd in the presence of water molecules, however, was found to be more heterolytic than in the vapor phase, forming products that have ionic characteristics. The dissociation of acetic acid over Pd(111) in the presence of solvating water molecules was calculated to be +37 kJ/mol. The metal surface stabilizes the acetate species but to a relatively weaker extent than the stabilization provided by the water solvent. The acetate anion was found to be 57 kJ/mol more stable when completely solvated by water molecules than on Pd(111). In the vapor phase, the acetate anion binds with an energy of over −198 kJ/mol on Pd(111). The surface acts as a "solvent" to shield the negative charge of the ion. In the presence of a solvent, however, the interaction between the acetate ion and the Pd(111) surface is weakened considerably. The interaction between acetate and the surface, however, is nevertheless attractive at −114 kJ/mol. While the acetate anion is thermodynamically more stable when completely solvated by water molecules, there appears to be a barrier for it to desorb from the metal surface.

1. Introduction

The presence of a solvent medium can significantly alter the thermodynamics and kinetics of surface-catalyzed reactions. Partially charged reaction intermediates that are not generally stable in the gas phase can exist in the solution phase and participate in the reaction chemistry. The local environment near the catalytic surface may therefore involve reactant molecules, products, reaction intermediates, various ions, and solvent molecules. The geometric and electronic structure of the surface reactant intermediates as well of the solvent network at the solid−liquid interface play an important role in dictating chemisorption energetics and the surface reactivity. Elucidating the effects of the detailed atomic structure at the solid−liquid interface could play an important role in tailoring solvent design in order to manipulate surface catalytic chemistry.

The complex nature of the solid−liquid interface, however, makes it a challenge to experimentally resolve relevant surface bound species and the effect of solvent on these intermediates.[1] In the 1980s, Sass and co-workers[2] pioneered a technique using ultrahigh vacuum to study the electrode−electrolyte interface in an electrochemical cell. The technique involves sequentially dosing a clean metal surface in vacuum with gas-phase molecules of the solvent, solute, and electrolyte ions. The metal surface is then analyzed using temperature-programmed desorption, low-energy electron diffraction, as well as a number of other relevant ultrahigh vacuum analyses to elicit information about the composition, structure, and energetics of the reaction intermediates. This technique has been used to study coadsorption of electropositive atoms such as Cs and K (model cations) as well as electronegative atoms such as Br and O (model anions) with water on Cu(110) and Ag(110) surfaces.[2−5] Stuve et al. have used ultrahigh vacuum (UHV) experiments to study adsorption of HNO_3/H_2O mixtures on Ag(110).[6] Nitric acid was observed to lose the proton to form a surface nitrate hydrogen-bonded to water molecules. Subsequently, Stuve et al. performed similar studies to understand the adsorption of $HClO_4$ and the interaction of water with adsorbed perchlorate and perchloric acid on Ag(110).[7] In a separate study,[8] UHV was used to examine "*specific*" and "*nonspecific*" modes of adsorption of perchlorate ion. An anion is considered "*specifically adsorbed*" if it is in direct contact with the metal surface and is "*nonspecifically adsorbed*" if it is fully solvated by water molecules and is not in direct contact with the metal surface. On the basis of the vibrational spectrum, the authors concluded that perchlorate ions exhibit nonspecific adsorption on Ag(110) at low surface coverages. However, very little is known from experiment about the structural details of adsorption of other complex ions at solution/metal interfaces.

Most theoretical modeling efforts in heterogeneous catalysis to date have focused on understanding chemisorption and surface chemistry for vapor-phase reactions. First principle quantum

* Author to whom correspondence should be addressed. E-mail: mn4n@virginia.edu.

10.1021/jp002797m CCC: $20.00
Published on Web 08/25/2001

chemical calculations have been shown to provide reliable predictions of adsorption and surface reaction energies in vapor-phase catalytic reactions with an accuracy that is on the order of 5 kcal/mol.[9] In recent years, there has been an increasing interest in using theoretical calculations to study homogeneous liquid-phase reactions. A good review of available theoretical techniques and their applications to homogeneous liquid-phase chemistry is provided by Cramer and Truhlar.[10] Traditionally, these studies have relied on using molecular mechanics and other semiempirical approaches to model the solvent medium. However, it is difficult to study reactions over extended metal surfaces using these methods due to the lack of accurate parameters for metals. More recently, Price and Halley[11] have pioneered a hybrid Car-Parrinello[12] type scheme which follows the molecular dynamics and density functional methods to study metal−electrolyte interfaces.

In this study our objective is to demonstrate the use of periodic density functional theory to obtain a microscopic understanding of the interaction of water molecules with adsorbates on metal surfaces and the role of water molecules in altering the adsorbate−metal interactions. Traditionally, periodic density functional theory has been used to provide a fundamental understanding of metal-catalyzed reactions in the vapor phase. We show that one can take first-principle quantum chemical methods further and begin to provide a fundamental understanding of metal-catalyzed reactions in the presence of solvent (water) molecules. This serves as an initial step toward developing an understanding of solvent effects in heterogeneous reaction chemistry. The explicit treatment of water molecules in our model offers an advantage over continuum models that have been used to examine solvent effects. The molecular level detail of the solute−solvent interactions, that is not available using continuum models, can be obtained using density functional theory. Though computationally intensive, periodic density functional theory also has merits compared to classical molecular dynamics approaches to examine the effect of solvation as it is not based on any empirical parameters to describe the metal surface.

Specifically, in this study we have examined the dissociative adsorption of acetic acid over Pd(111) in the presence of water as a solvent medium. The dissociation of acetic acid is one of the first steps in the synthesis of vinyl acetate and therefore has direct industrial relevance. This chemistry is generally carried out in the liquid phase. The mechanism for this reaction and the role of solvent, however, are still relatively unknown. In fact, little is known about the fundamental mechanisms of most solvated metal−surface reactions. This study was undertaken to begin to provide insights in to the metal-catalyzed dissociation of acetic acid in a solvating environment.

Slab calculations allow us to create a three-dimensional solution environment using explicit water molecules. A unit cell containing a finite number of solute molecules, metal atoms, and solvent molecules is repeated periodically in space to generate a large three-dimensional lattice. Sufficient care is exercised in building the unit cell so that water molecules between adjacent unit cells align in such a way to form hydrogen bonds. This sets up a three-dimensional network of hydrogen-bonded water molecules similar to that observed in bulk water. By using the periodic super-cell approach, we have implicitly assumed that the solvent structure is crystalline. It may be argued that while the solution medium involves a random network of solvent and solute molecules, the imposition of periodic boundary conditions may seem inappropriate. However, by choosing a sufficiently large unit cell that contains a large number of solvent molecules, it may be possible to introduce enough randomness to appropriately capture the first-order effects of solvation on the structure and energetics of the reaction intermediates at the metal interface. It is also well established that solutes and solvent molecules such as water form well-ordered structures in the vicinity of crystalline metal surfaces.[13] As one moves away from the metal surface, the arrangement of solvent molecules is more random as in a bulk solution. Since we are interested in modeling reactions that occur within a few angstroms of the metal surface, the imposition of crystallinity may work out to be a reasonably good approximation.

Water is a liquid at modest temperatures with many possible iso-energetic conformations. Using periodic DFT optimization scheme, we have likely captured just one snapshot of the equilibrium structure of water. Water, however, is not a static structure. To follow the free energy changes associated with the reaction would require ab initio MD simulations which would enable us to follow the changes in the transition state structures and their effects on catalytic activity and selectivity. We have used periodic density functional theory primarily to extract information on the energetics of metal-catalyzed deprotonation reaction in the presence of water molecules. We have not commented on the associated entropic changes and have laid little emphasis on the entropic effects or the structural details of water. In the case of deprotonation of acetic acid in the presence of water molecules, we have examined two completely different arrangements for the water molecules. Both the arrangements of water molecules give the energy of deprotonation of acetic acid within 2.3 kJ/mol of each other. We have also performed ab initio MD calculations at 300 K to reexamine the deprotonation of acetic acid over Pd(111) in the presence of water. The MD study is not meant to follow the dynamics of the reaction, but to see how the energetics are affected by the presence of a solvent. The geometries obtained using periodic DFT optimization were used as input structures for the ab initio MD. Up to about 0.5 ps of the MD run, we find little change in the electronic energy from the values computed using the traditional optimization schemes. Our analysis and conclusions, which are based only on the computed electronic energies therefore, stand.

2. Computational Details

All calculations reported in this paper were performed using density functional theory plane wave code, DACAPO,[14] developed at the Denmark Technical University. Dacapo is a nonlocal gradient-corrected pseudopotential DFT code based on the developments of Payne, Teter, and co-workers[15] and of Gillan[16] to solve the Kohn Sham equation[17] in a basis of plane waves. A cut-off kinetic energy of 40 Rydberg was used to make the plane wave basis set finite. This cut-off of 40 Rydberg was found sufficient to attain convergence in the calculated adsorption and reaction energies. Increasing the cut-off energy to 60 Rydberg produced less than 0.03 eV change in the relative energies. The electronic states were computed at 18 special k-points in the first Brillouin zone. The k-points were chosen by the method of Chadi and Cohen.[18] 18 Chadi Cohen k-points are found sufficient to describe a $\sqrt{3} \times \sqrt{3}$ unit cell of a Pd(111) slab. Increasing the k-point grid size from 18 to 54 produces less than 0.01 eV change in the electronic energy. The Perdew Wang (PW91) functional was used within the Generalized Gradient Approximation (GGA)[19] to describe non local exchange and correlation effects. Non local gradient corrections were required since the local density approximation (LDA)[20,21] is reported to be inaccurate for describing weakly bonded

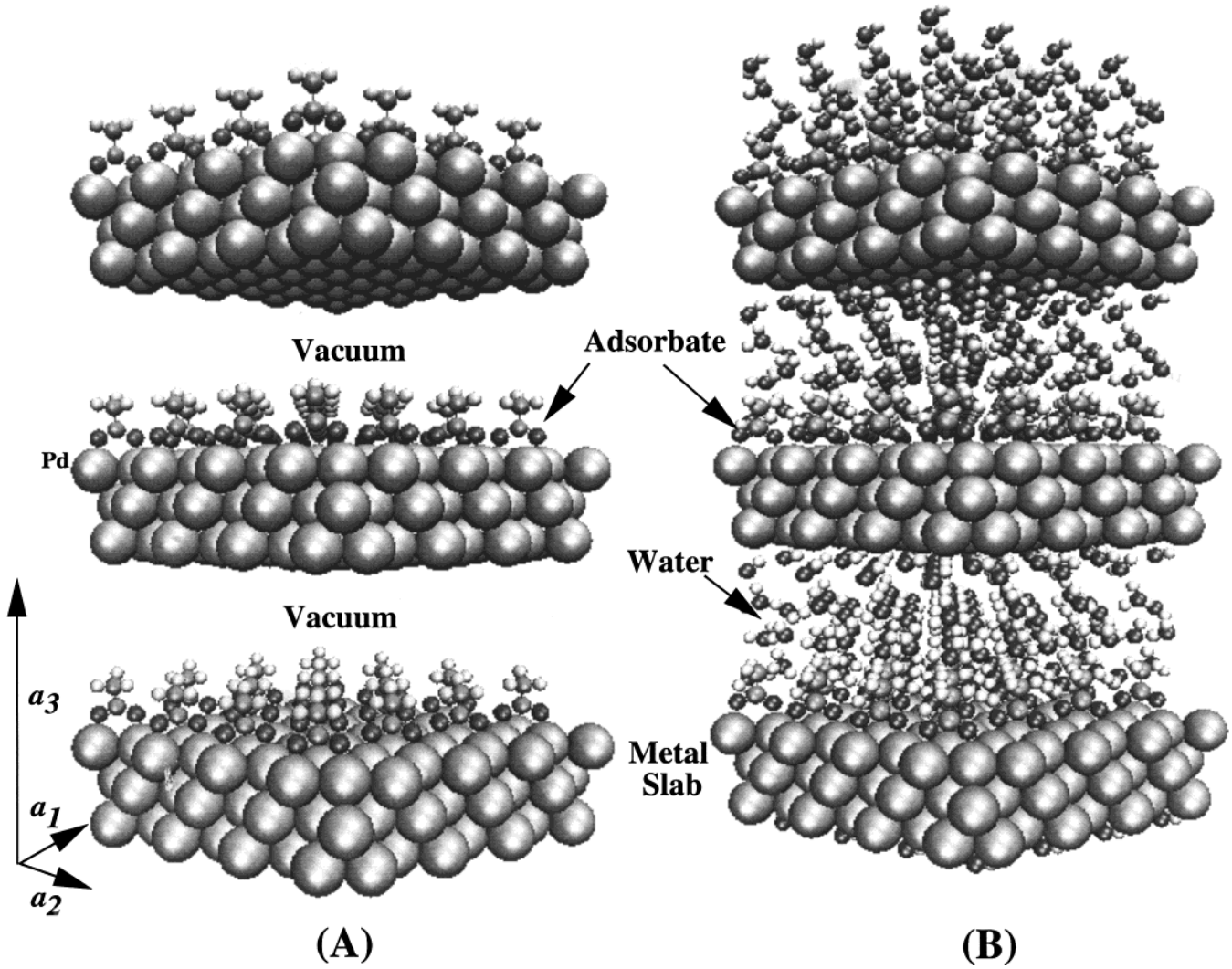

Figure 1. Geometry set up for periodic slab DFT calculations. Four unit cells are shown in a_1 and a_2 directions and three unit cells in the a_3 direction. (A) Vapor-phase adsorption: Each unit cell consists of three layers of Pd(111), an adsorbate, and a vacuum region in the a_3 direction; (B) Adsorption in the presence of water: Each unit cell consists of three layers of Pd(111), the acetate adsorbate, and water molecules that completely fill in the vacuum region.

systems such as the hydrogen-bonded network of water molecules.[22,23] Frozen core, scalar relativistic, norm conserving pseudopotentials of Troullier and Martins[24] were used to describe all the core electrons.

A damped verlet molecular dynamics algorithm was used to initially establish the hydrogen-bonded network between water molecules. This algorithm better samples phase space and was used to lower the forces on individual atoms. Once the system was brought close to the minimum, we switched to a conjugate gradient optimization scheme to fine-tune the system geometry and energy. To help ensure that we have found a relative minimum, we have performed geometry optimizations starting with a few different initial guess structures. All the guess structures arrived at the same final geometry on optimization, indicating that the final structure represents a deep local minimum. For example, in Section 4.5.2 we find that the proton on optimization tends to be separated from the adsorbed acetate species by only one water molecule, irrespective of whether it was separated from the acetate species by five, three, or one water molecule in the starting structure.

A schematic representation of the periodic lattice structure used in all calculations described herein is shown in Figure 1. A defined unit cell is translated in space in three dimensions to generate the overall system. a_1, a_2, and a_3 denote the translation vectors. Figure 1A,B shows four unit cells along the a_1 and a_2 vectors (*XY* plane) and three unit cells (slabs) along the a_3 vector (*Z* direction). A $\sqrt{3} \times \sqrt{3}$ super cell was used to model the interactions of acetic acid, acetate, and water with the Pd surface. Acetate is known to order in a $\sqrt{3} \times \sqrt{3}$ arrangement on the Pd(111) surface under UHV conditions.[25] The unit cell consists of three layers of Pd(111) atoms. In a previous study,[26] the effect of the number of metal layers on the adsorption energy of H atom over Pd(111) was examined. The adsorption energy was observed to be invariant beyond three Pd layers for a fairly strong adsorbate like the hydrogen atom. The effect of the number of metal layers will be less important for weaker adsorbates such as water which produce very little relaxation in the metal. Therefore, three layers are sufficient to model Pd(111) in this study. The lattice constant of the metal has been optimized by performing a series of calculations on bulk palladium. The equilibrium lattice constant is calculated to be 3.89 Å. This is in direct agreement with the experimental lattice constant of Pd (3.89 Å). Since close packed fcc metal surfaces undergo little relaxations during adsorption,[27] the palladium atoms constituting the (111) surface were initially held fixed during geometry optimization. Once the optimal geometry of

the adsorbate was determined, the first two layers of palladium atoms were allowed to relax. As expected, in most cases, interlayer relaxations were small and caused a change of less than 2 kJ/mol in the electronic energy of the system.

Density functional theory cluster calculations were also performed using Gaussian 94[28] to examine the effects of liquid clusters on the dissociation of acetic acid in the absence of Pd. The internal geometry of each water molecule as well as the structural arrangement of the networked water molecules were optimized using 6-31G(d) basis sets. The B3LYP[29] three parameter hybrid functional was chosen to describe the exchange and correlation functionals since it is reported to be reliable in studying multiple hydrogen bond systems.[30] The B3LYP functional includes Becke's gradient corrections[31] to LDA exchange and Lee, Yang, and Parr's gradient corrected correlation functional.[32]

3. Calculation Scheme for Vapor-Phase and Solvent-Phase Calculations

Figure 1A shows the structural set up for the vapor-phase calculations. The super cell consists of a finite number of metal atoms, the adsorbate, and a vacuum region. It is translated in space along a_1, a_2, and a_3 directions to generate an infinite number of slabs stacked up one above the other and separated by a vacuum region. The vacuum region was chosen to have a thickness that corresponds to eight metal layers in order to separate the slabs along the a_3 vector.

The adsorption energies of adsorbates in the "vapor phase" were computed using eq 1:

$$\Delta E_{\text{adsorption}} = E_{\text{adsorbate/Pd(111)}} - E_{\text{adsorbate}} - E_{\text{Pd(111) slab}} \quad (1)$$

where $E_{\text{adsorbate/Pd(111)}}$ = total SCF energy of adsorbate bound to the Pd(111) surface, $E_{\text{adsorbate}}$ = total SCF energy of an isolated adsorbate, and $E_{\text{Pd(111)slab}}$ = total SCF energy of bare Pd(111) slab.

Figure 1B depicts the repeated unit cell for modeling solvent effects on the interaction of acetate with the metal surface. The key difference between the liquid-phase and vapor-phase calculation setup is the addition of water molecules to solvate the acetate surface intermediate. The acetate intermediate is allowed to interact with the top layer of the palladium surface. Water molecules fill in the vacuum region between the metal slabs. For our calculations, we have chosen eight water molecules per unit cell to represent the solvent. At least eight water molecules are necessary to allow for formation of hydrogen bonds between all water molecules within a unit cell and between water molecules in adjacent unit cells. In some cases we have verified that eight water molecules in the unit cell are adequate to provide a good description of the energetic effects of solvating water molecules on the chemistry of interest. For example, we have examined the deprotonation of acetic acid in water (without metal) using 7, 8, and 12 water molecules. The deprotonation energy changed by a little over 3 kJ/mol by increasing the number of water molecules from 7 to 8 and by less than 1 kJ/mol in changing from 8 to 12 water molecules. We have also examined the deprotonation of acetic acid over Pd(111) in water using 7, 8, and 9 water molecules in our model. All these models gave deprotonation energies within 3.0 kJ/mol of each other. In our model, some of the water molecules are allowed to interact with the bottom layer of the palladium slab, thus completely eliminating the vacuum region. The metal atoms in the bottom layer were held fixed at their bulk positions. This is reasonable because adsorption of a weak species such as water produces little relaxation in the metal surface. The water molecules form a three-dimensional network of water−water hydrogen bonds, metal−water bonds, and water−adsorbate hydrogen bonds.

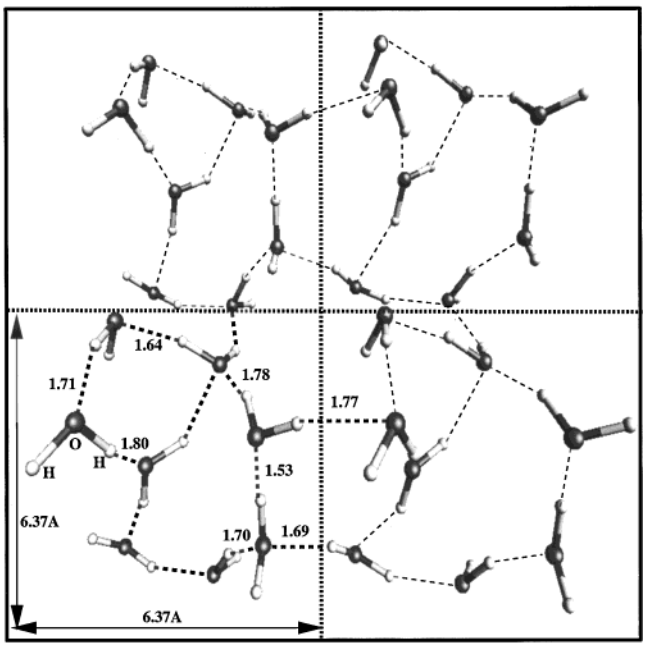

Figure 2. Periodic DFT optimized structure of bulk water. Four identical unit cells are shown projected in to the plane of paper. The image has been slightly rotated to clearly show the hydrogen-bonded network in water. The hydrogen bonds are shown by dotted lines.

4. Results and Discussions

4.1. Water. As a first step toward modeling the hydrogen-bonded network in water, we performed periodic DFT calculations on water−without any solute molecules or metal atoms. A cubic unit cell containing eight water molecules was chosen to represent the system. As an initial guess, the dimensions of the cube were fixed at 6.21 Å each. This value was chosen so that the density of water in the unit cell is approximately 1 g/cc. The structural locations of all eight water molecules were optimized and the total electronic energy of the system was determined at the ground state. The calculations were then repeated by optimizing the geometry for varying sizes of the unit cell. The total SCF electronic energy of the system was found to go through a minimum at unit cell dimensions of 6.37 Å × 6.37 Å × 6.37 Å. Since there are eight water molecules in every unit cell of these dimensions, the density of water in the unit cell is calculated to be 0.925 g/cc. Figure 2 shows four identical unit cells of the optimized system. The hydrogen bonds are depicted by dotted lines. We consider two water molecules to be hydrogen-bonded if the O−O distance between the two water molecules is less than 3.35 Å and the angle between the intramolecular O−H vector and the intermolecular O−O vector is smaller than 20°. This definition of hydrogen bonding has been previously applied by Heinzinger and Palinkas[33] to describe the properties of bulk aqueous systems. Hydrogen bonds are formed between water molecules of the same unit cell as well as between water molecules of adjacent unit cells. On an average, each water molecule is observed to form two hydrogen bonds. The length of the hydrogen bonds varies between 1.53 and 2.11 Å. The longer distances were typically observed for two hydrogen bonds that share an oxygen atom (Figure 3). The shorter distances were typically associated with oxygens which form only a single hydrogen bond.

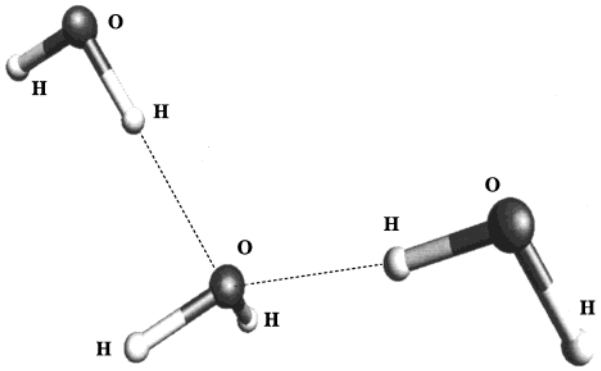

Figure 3. Schematic representation of two hydrogen bonds sharing an oxygen atom.

The total SCF energy for a network of water molecules calculated per water molecule is lower than the total SCF energy of an isolated water molecule by 40 kJ/mol. This lowering of energy is due to the formation of hydrogen bonds between water molecules. Since each water molecule on an average is involved in two hydrogen bonds, the strength of a hydrogen bond in water is calculated to be 20 kJ/mol. This is in agreement with the experimental data summarized by Eisenberg[34] that estimates the strength of hydrogen bond in water and ice to be between 15 and 25 kJ/mol. The agreement of our results for the structure and energetics of water with experimental observations helps to begin to validate the use of periodic DFT calculations for understanding chemistry in the solution phase.

4.2. Deprotonation of Acetic Acid. To distinguish the effects of the metal as well as the water solvent on the deprotonation of acetic acid over palladium we examined acetic acid in the four following environments: (1) gas phase (in the absence of both the metal and the solvent), (2) solvent phase (in the presence of water but the absence of the metal), (3) vapor phase over the metal (in the absence of water), and (4) liquid phase over the metal (presence of both water and the metal).

Throughout the discussion we use the term "gas phase" to describe reactions occurring in a vacuum without any metal surface. The term "vapor phase" is used to describe the metal-catalyzed reactions in a vacuum.

4.2.1. Gas Phase. The heterolytic dissociation of acetic acid produces an acetate ion along with a proton.

$$CH_3COOH \rightarrow CH_3COO^- + H^+ \qquad (2)$$

The energy associated with the deprotonation of acetic acid is also the value of the proton affinity of the acetate anion. The proton affinity of the acetate anion is reported to be 1471 kJ/mol based on mass spectrometry and thermodynamics.[35] DFT cluster calculations estimate the deprotonation energy of acetic acid in the gas phase to be +1483.2 kJ/mol. The DFT result for the deprotonation of acetic acid is thus in good agreement with the known experimental value. The extremely high reaction endothermicity is expected since the gas-phase dissociation reaction involves the heterolytic scission of a stable acetic acid molecule to two oppositely charged (cation and anion) unstable fragments. The same reaction, on the other hand, can occur quite readily in solution. This is due to the stabilization of the ionic fragments from solvation.

4.2.2. Effect of Solvation on Deprotonation of Acetic Acid. DFT cluster calculations were performed to examine the effect of individual water molecules on stabilizing the reactants and products of acetic acid deprotonation in the gas phase. When a single water molecule is involved, it may be associated with either the acetate anion or with the proton in the product state. Therefore, both of these cases are examined below in eqs 3 and 4:

$$CH_3COOH\cdot H_2O \rightarrow CH_3COO^-\cdot H_2O + H^+ \qquad \Delta E = +1436 \text{ kJ/mol} \quad (3)$$

$$CH_3COOH\cdot H_2O \rightarrow CH_3COO^- + H_3O^+ \qquad \Delta E = +869 \text{ kJ/mol} \quad (4)$$

The addition of a single water molecule lowers the endothermicity of the reaction from +1483 kJ/mol in the gas phase to either +1436 kJ/mol when the acetate anion is stabilized and to +869 kJ/mol when the proton is stabilized by water. The presence of a single water molecule is significantly pronounced when it is associated with the proton. In the case of the bare proton, the positive charge is localized at a single nuclear center. Association of the proton with a water molecule to form H_3O^+ begins to delocalize the positive charge and hence stabilizes the proton. Water has a similar effect in stabilizing the charge on an acetate ion. However, the effect is less pronounced since the charge on a bare acetate ion is initially more delocalized than that of the bare proton.

Periodic slab calculations were used to study the deprotonation of acetic acid in the presence of many water molecules. The reactant and product geometries for acetic acid deprotonation are shown in Figure 4. The shape and size of the unit cell used to examine acetic acid deprotonation were identical to that used to simulate water in Section 4.1. Figure 4 shows four unit cells for this system. There are eight explicit water molecules in the unit cell all of which hydrogen bond. They also form hydrogen bonds with their images in the adjacent cells. During geometry optimization of the reactant and product states, the water molecules oriented in space to form an optimal network. The calculations for the dissociated H^+ and CH_3COO^- entities were performed spin-unpolarized. This is a reasonable approximation in that in the heterolytic dissociation of acetic acid into an acetate ion and a proton, all electrons are paired. It was verified at the final structure of the optimized state that no eigen-state had an unpaired electron. Unpaired electrons would imply that the dissociation products are free radicals ($CH_3COO\cdot$ and $H\cdot$) rather than ions (CH_3COO^- and H^+).

In the case of acetic acid, it is seen that the hydrogen bond that forms between the proton of an acetic acid molecule with the hydroxyl oxygen on a neighboring water molecule is shorter than all other hydrogen bonds in the system. This is expected since the Brönsted acidity of the hydrogen atom of acetic acid is comparatively greater than that of water. For the deprotonated product case, the proton in solution was observed to exist as an $H_5O_2^+$ like species embedded in a network of water molecules. The geometry of the $H_5O_2^+$ species is shown in Figure 4B. The O−O bond distance in $H_5O_2^+$ was observed to be 2.52 Å with the proton located between the two oxygen atoms. The H^+−O bond distances are 1.05 and 1.50 Å. The acetate ion was surrounded by water molecules that formed comparatively short hydrogen bonds with its oxygen atoms ranging from 1.51 to 1.69 Å. The hydrogen bonds between the water molecules ranged from 1.73 to 1.86 Å.

DFT periodic slab calculations suggest that the energy of deprotonation of acetic acid in water is +4.0 kJ/mol. The experimental value for the energy of deprotonation of acetic acid in water is −0.57 kJ/mol.[36] This difference of 4.5 kJ/mol between the theoretical and experimental values for the deprotonation energy of acetic acid in water is within the current

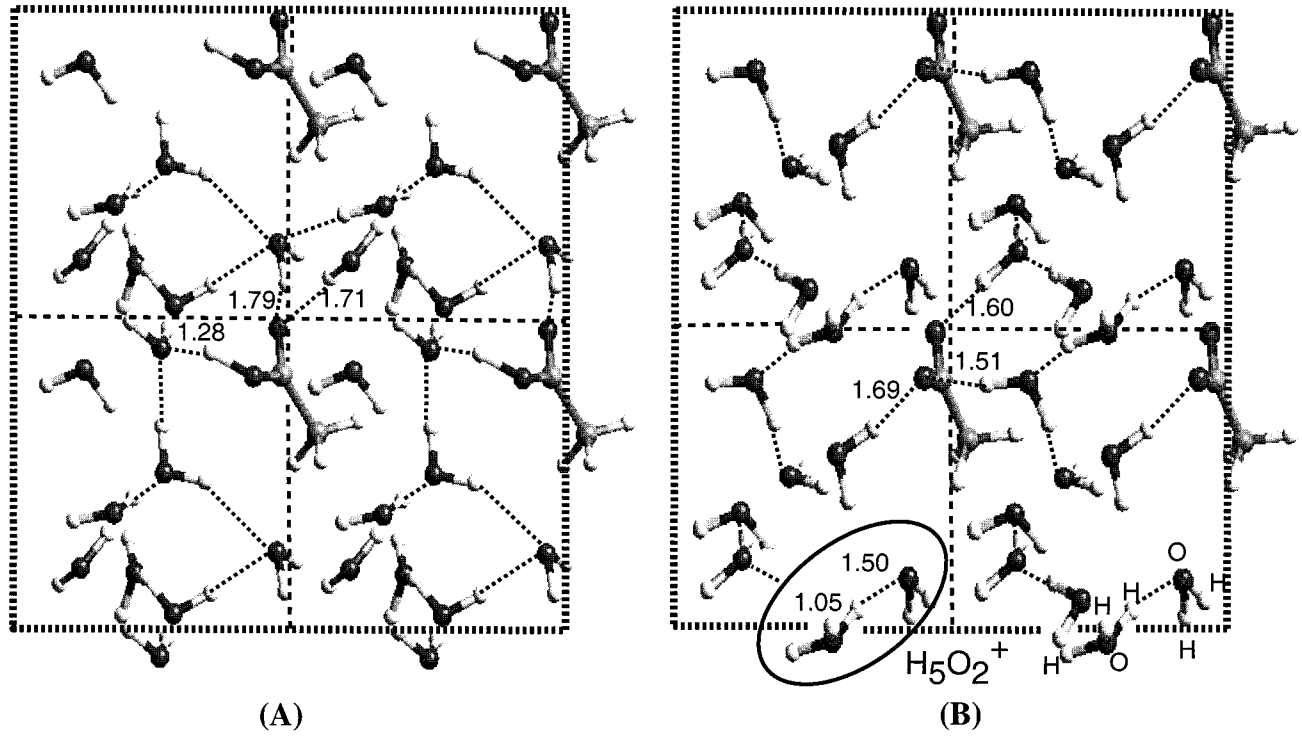

Figure 4. DFT periodic slab optimized geometry for (A) acetic acid in water; (B) acetate(−), and H(+) solvated by water.

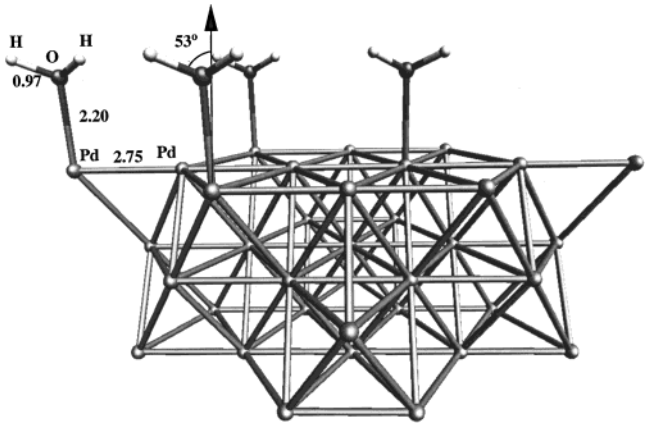

Figure 5. DFT periodic slab optimized geometry for vapor-phase adsorption of water ($\sqrt{3} \times \sqrt{3}$) on Pd(111).

accuracy of the DFT methodology (20 kJ/mol). In comparison to the gas-phase deprotonation of acetic acid, where the reaction is highly endothermic (+1483 kJ/mol), the dissociation in water is almost thermoneutral (+4.0 kJ/mol). This is because water strongly stabilizes the charged fragments formed by deprotonation. The fragments are highly unstable when formed in the gas phase.

4.3. Adsorption of Water on Pd(111). The metal surface can also stabilize the fragments formed by deprotonation of acetic acid. In our present study, we have investigated the deprotonation of acetic acid over the Pd(111) surface and the role of solvent in the deprotonation over the metal surface. The solvent molecules can alter the energetics of the deprotonation of acetic acid on the metal. Water molecules from the solvent can compete with acetic acid for adsorption sites on the Pd(111) surface, thereby reducing the number of surface sites available for the adsorption of acetic acid.

4.3.1. Vapor-Phase Adsorption. Figure 5 shows the geometry of a water molecule adsorbed on a Pd(111) slab in the vapor phase. Water adsorbs via van der Waals attractive interactions between one of the lone pairs of electrons on the oxygen and the empty states in the d-band of the metal. The extra lone pair of electrons on the oxygen atom orients the adsorbed water into a tilted configuration whereby oxygen takes on sp^3 symmetry. The Pd−O bond distance is about 2.20 Å long. The molecular plane of water is slightly tilted away from the plane of the surface. The plane of the water molecule makes an angle of 53° with respect to the surface normal. A similar orientation of water on Pd(100) was reported by Andersson et al.[37] using electron energy loss spectroscopy (EELS). Water is a weak adsorbate on the palladium surface. We calculate the adsorption energy of water on Pd(111) to be −30 kJ/mol. Based on temperature-programmed desorption of Stuve and Madix[38] for water on Pd(100) and assuming first-order desorption with a preexponential factor of 1×10^{13} s^{-1}, the experimental binding energy of water on Pd(100) is estimated to be −43 kJ/mol.

4.3.2. Effect of Solvation on Adsorption of Water. Figure 6 shows the adsorption of water on a Pd(111) surface in the presence of excess water molecules that solvate the adsorbed water surface species. The optimized structure indicates that the water molecules orient in space to form a network of hydrogen bonds. The adsorbed water molecule interacts with the palladium surface through its oxygen atom. Our calculations indicate that the water molecules which were adsorbed tilted with respect to the metal surface in the vapor-phase H_2O/Pd(111) system, now sit nearly parallel to the metal surface. Molecular simulations by Spohr show a very similar conformation for the water/Pt(111) interface.[39] Our calculations suggest that the Pd−O distance for water/Pd(111) is 0.1 Å longer when the adsorbed water is solvated by other water molecules. The interaction of the adsorbed water molecule with the Pd(111) surface is weakened when the water molecule forms hydrogen bonds with the solvating water molecules.[13]

As shown in the Figure 6 for multilayer adsorption of water on Pd(111), adsorbed water molecules form hydrogen bonds with water molecules in the second layer. The second layer of water molecules in turn is hydrogen bonded to the adsorbed

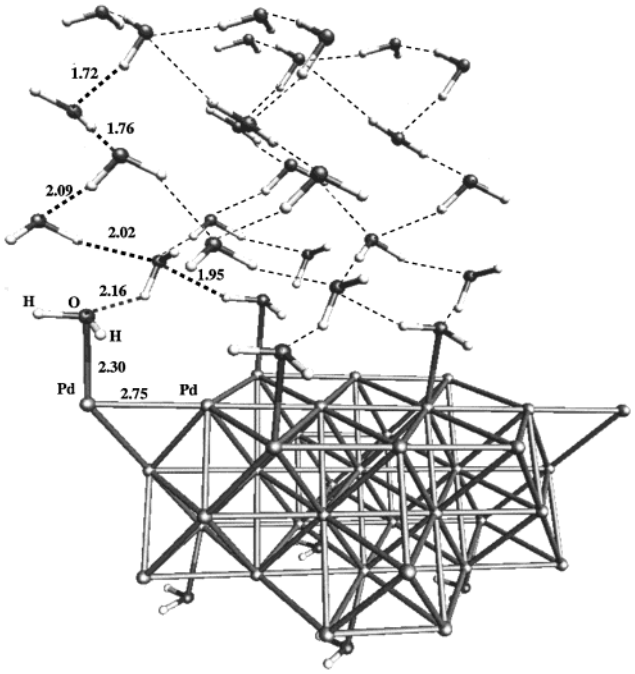

Figure 6. Periodic DFT optimized geometry for multilayer adsorption of water on Pd(111) in the presence of water.

water molecules and to the next layer of water molecules. The resulting adsorption configuration found here is quite similar to the "bilayer" model proposed by Doering and Madey.[40] The model was proposed on the basis of their analysis of adsorption of water on Ru(0001) studied using thermal desorption spectroscopy (TDS), low-energy electron diffraction (LEED), and electron stimulated desorption ion angular distribution (ESDIAD). The water molecules close to the metal surface pack in a $\sqrt{3} \times \sqrt{3}$ surface structure due to the influence of adsorption on the crystalline metal surface. This arrangement of water molecules, however, loses its orientation with respect to the metal surface as one moves away from the surface, thus becoming less crystalline away from the surface.

Because water which is adsorbed to the metal surface also interacts with solvating water molecules, the water−metal interaction is expected to be weaker than that for the vapor-phase H_2O/Pd(111) system. The general equation for adsorption given as eq 1 is adapted to determine the interaction of water on Pd in a water solution. For the solvated case, the adsorbed water molecule along with all solvating water molecules was treated as the "*adsorbate*". The geometric structure of the "*adsorbate*" was independently optimized to determine the term $E_{\text{adsorbate}}$ in the RHS of eq 1. The first term, $E_{\text{adsorbate/Pd(111)}}$ of eq 1 refers here to the total electronic energy for multilayer adsorption of water on Pd(111). Our calculations indicate that the interaction energy for a single water molecule with the Pd(111) surface in the presence of other water molecules is nearly thermoneutral. We have accounted for interaction of two water molecules with the Pd(111) surface per unit cell—one water molecule interacts with the top layer of Pd(111) slab and the other with the bottom layer of the slab. Here, the water−Pd(111) interaction energy computed as above is −2.5 kJ/mol. Bange et al. have studied multilayer adsorption of water on Ag(110) using thermal desorption spectroscopy.[41] They report that the water−water bond breaking and water−metal bond breaking steps peaked at the same temperature in the spectrum. This indicates that the strength of the multilayer water−water interaction is nearly the same as water−metal interaction, leading the authors to conclude that there is no net driving force for bulk water to adsorb directly on Ag(110).

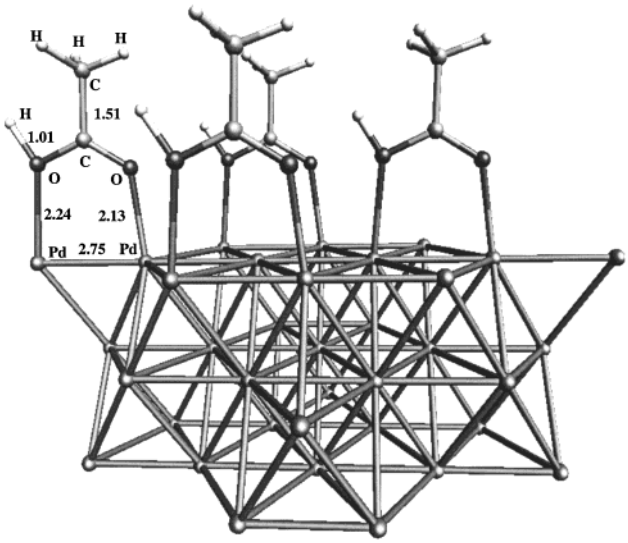

Figure 7. DFT optimized structure for the $(\sqrt{3} \times \sqrt{3})$ periodic vapor-phase adsorption of acetic acid on Pd(111) 3-layer slab.

4.4. Adsorption of Acetic Acid. The first step in the deprotonation of aqueous acetic acid on Pd(111) surface is the adsorption of acetic acid from the solution on the metal surface. The adsorbed acetic acid can subsequently dissociate on the metal surface into acetate and hydrogen intermediates.

4.4.1. Vapor-Phase Adsorption. An isolated acetic acid molecule is very weakly bound to the Pd(111) surface. The interaction energy of acetic acid with the metal surface is calculated using DFT slab calculations to be −25 kJ/mol. The experimental value indicates that acetic acid adsorption is stronger at −49.8 kJ/mol,[25] but this is the result of catemar formation or local hydrogen bonding in the chemisorbed overlayer. The preferred mode of adsorption of acetic acid on Pd(111) is shown in Figure 7. Acetic acid sits di-σ on the palladium surface, interacting with the metal atoms through both of its oxygen atoms. The mode of adsorption, as was the case with water, involves a van der Waals interaction between the lone pair of electrons on oxygen and the metal surface. The Pd−O distances are 2.24 and 2.13 Å, the longer distance being for the oxygen atom which is also bound to the acidic hydrogen atom. The C−C bond is oriented perpendicular to the metal surface.

4.4.2. Effect of Solvation by Water Molecules. The adsorption of acetic acid on Pd(111) in the presence of water was examined again by adding eight water molecules into the acetic acid/Pd(111) unit cell. The water molecules are initially placed around the adsorbed acetic acid species in order to set up a solvation shell. The optimized geometry for this system is shown in Figure 8. The optimized solvent molecules are oriented in space to form hydrogen bonds between molecules of the same unit cell as well as with adjacent unit cells. Similar to the structure of water described in Section 4.1, each water molecule on average participates in forming two hydrogen bonds. The length of the hydrogen bonds between the water molecules was found to vary from 1.47 to 1.79 Å. The hydrogen bond formed between the proton of acetic acid and a neighboring oxygen atom of water was 1.32 Å. Acetic acid binds to the palladium surface in a di-σ configuration through the oxygen atoms. This is similar to the adsorption mode found for the vapor-phase adsorption of acetic acid. However, the Pd−O distances are now 2.35 and 2.18 Å, which are 0.11 and 0.05 Å longer than the

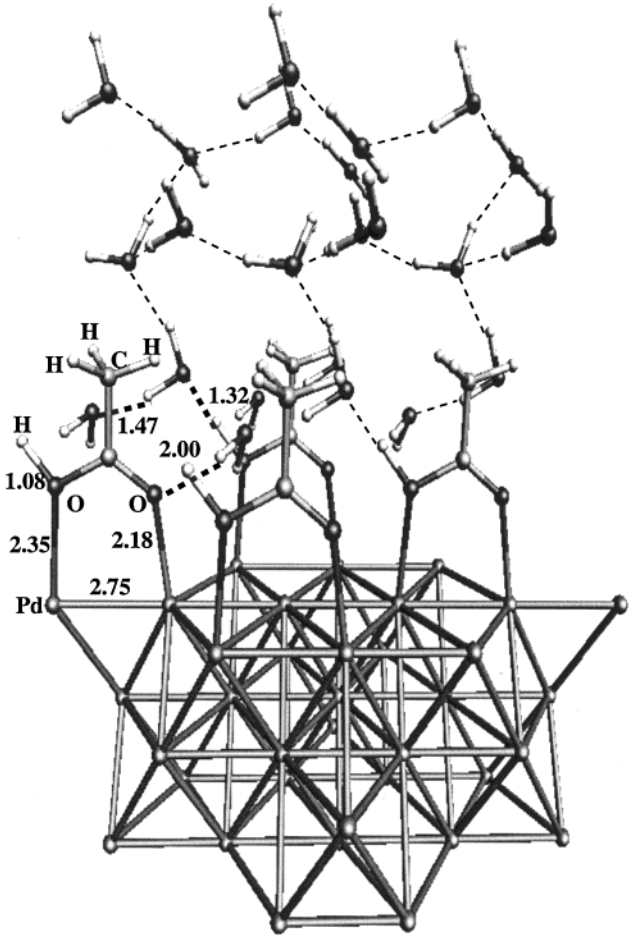

Figure 8. Periodic DFT optimized geometry of acetic acid adsorbed on 3-layer Pd(111) in the presence of solvating water molecules.

vapor-phase adsorption of acetic acid. This is because the acetic acid can now form hydrogen bonds with the water molecules that sit above it. Interactions with the water molecules would be expected to weaken the interaction of acetic acid with the Pd(111) surface.

4.5. Dissociation of Acetic Acid on Pd(111). Acetic acid molecules adsorbed on the metal surface can dissociate to form the acetate and hydrogen intermediates.

4.5.1. Vapor-Phase Dissociation. Adsorbed acetic acid on Pd(111) is known to dissociate readily to form surface bound acetate and a hydrogen intermediate. Figure 9 depicts the binding of acetate on the Pd(111) surface in the vapor phase. The geometry of adsorbed acetate is somewhat similar to that of acetic acid on Pd(111). Acetate preferentially adsorbs in a di-σ adsorption mode, interacting with the metal surface through its oxygen atoms. These results are consistent with our previous cluster calculations which indicate that acetate in the di-σ mode is over 120 kJ/mol more stable than the mono and bidentate modes.[42] The evaluated frequencies for the di-σ mode agree quite well with the HREELS data by Davis and Barteau[25] who also suggest the di-σ adsorption mode. In contrast to acetic acid, the two oxygen atoms of acetate are identical and hence the calculated Pd−O bond distances are nearly of the same length (2.11 and 2.13 Å). The binding energy of acetate on Pd(111) was computed to be −198 kJ/mol using DFT calculations. Unlike acetic acid, which is a stable species as an isolated molecule, the acetate species is not stable as an isolated fragment. Hence, the interaction of acetate with Pd(111) is significantly stronger than that for acetic acid.

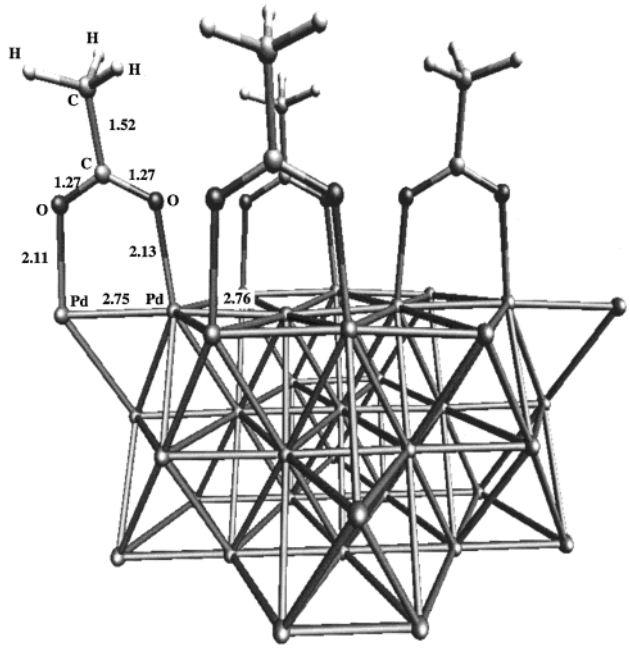

Figure 9. DFT optimized structure for the ($\sqrt{3} \times \sqrt{3}$) adsorption of the acetate intermediate on the Pd(111) slab.

The hydrogen atom formed as a result of dissociation of acetic acid also forms strong bonds with the metal surface. It is most favorably bound to the Pd(111) surface in the 3-fold fcc hollow site. The interaction energy of the hydrogen atom with the metal was computed using DFT calculations to be −266 kJ/mol at 33% coverage. This is in close agreement with the interaction energy of hydrogen atom with Pd(111) calculated by Neurock et al.[26] (−257 kJ/mol) and by Sautet et al.[43] (−260 kJ/mol).

The energy for the dissociation of acetic acid in the vapor phase over Pd(111) into the acetate and hydrogen surface intermediates is calculated to be +28 kJ/mol. The dissociation of acetic acid over the metal surface is less endothermic than the homolytic dissociation of acetic acid into acetate and hydrogen radicals in the gas phase (+468 kJ/mol). The metal surface lowers the overall energy for the deprotonation of acetic acid by stabilizing the reaction products. The charges on each of the atoms in the unit cell were calculated using a Mulliken analysis of the charge distribution. Notwithstanding the known deficiencies in the Mulliken charges, we compared the calculated charges to known, gas-phase free radical and ionic systems in order to estimate whether the intermediates were more free radical or ionic. The adsorbed acetate and hydrogen intermediate on Pd in the vapor phase were found to be more free radical like than ionic. The adsorbed acetate intermediate carries a charge of 0.20 units greater than the acetate free radical while the hydrogen atom gains a charge of 0.14 units on adsorption.

4.5.2. Effect of Solvation by Water on Acetic Acid Deprotonation over Pd(111). The dissociation of adsorbed acetic acid on Pd(111) in the presence of solvating water molecules, takes on more ionic like characteristics and therefore can be written as

$$(CH_3COOH)_{ads/aq} \rightarrow (CH_3COO)^-_{ads/aq} + H^+_{ads/aq} \quad (5)$$

This is in contrast to the vapor-phase dissociation of acetic acid over Pd(111) which is much more free radical like.

In eq 5, $(CH_3COOH)_{ads/aq}$ denotes acetic acid bound to the Pd(111) surface in the presence of water, $(CH_3COO)^-_{ads/aq}$ denotes acetate bound to Pd(111) in the presence of water and

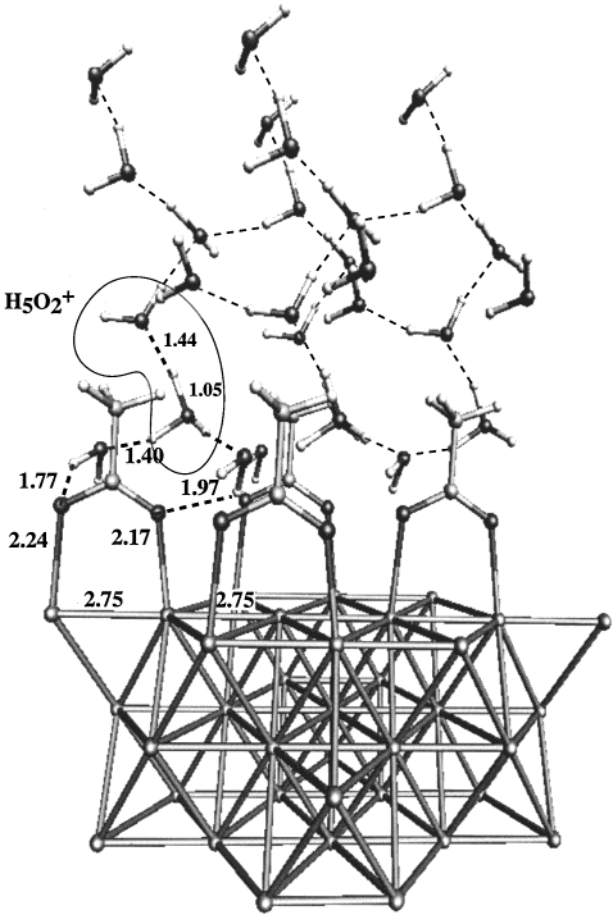

Figure 10. Deprotonated acetic acid adsorbed on Pd(111) and solvated by water molecules.

$H^+_{ads/aq}$ denotes proton at the interface in the presence of water. We find that the proton that is formed prefers to sit removed from the surface as an $H_5O_2^+$ intermediate. Thus the term $H^+_{ads/aq}$ is really H^+_{aq}. Kizhakevariam and Stuve[44] have considered the reaction 6 between a hydrogen atom bound to Pt(111) surface and water to form aqueous hydronium ion (H_3O^+).

$$H_{(ad)} + H_2O \rightarrow H_3O^+_{(aq)} + e^- \qquad (6)$$

They report the formation of aqueous hydronium ion from surface bound hydrogen and water to be energetically thermoneutral.

Figure 10 shows the optimized geometry of the products formed by deprotonation of acetic acid over Pd(111) in water. Acetate which is formed by the deprotonation of acetic acid in the presence of water binds in a di-σ configuration on Pd(111). This is very similar to the geometry of an isolated acetate on Pd(111) in the vapor phase.

The proton was observed to exist as an $H_5O_2^+$ species embedded in a network of water molecules. We have performed the optimization starting with three different positions of the proton with respect to the adsorbed acetate species. In the three initial structures, the proton was separated from the acetate species by 1, 3, and 5 water molecules, respectively. On performing geometry optimization, all three starting geometries lead to the same final structure. The proton was observed to migrate through water molecules in the course of optimization and finally resides close to the acetate species separated by one water molecule. The migration of the proton between the water molecules occurred by a successive sequence of proton transfer steps between the water molecules that form a network. This can be viewed essentially as proton conduction:[45]

$$(H_2O)-H^+\cdots OH_2 \rightarrow (H_2O)\cdots H^+-(OH_2)$$

A critical factor in the relaxation scheme is the choice of "time step" for ionic update. The time step here, as in other periodic DFT calculations, refers to the numerical time step of integration. It is used only to converge the geometry and does not pertain to actual dynamical motion such as in an actual MD simulation. A low time step is useful to identify shallow energetic minima and small barriers on the potential energy surface. A large time step causes faster convergence but may skip shallow energetic minima. It is useful to find deeper wells on the potential energy surface. To avoid being locked in to the many possible shallow minima on the potential energy surface of water, we have used a large time step for geometry optimization and consequently, could observe the migration of protons between water molecules. When we reexamined the optimization with a low time step for ionic update, however, we did not observe the migration of protons between water molecules. This suggests that there is a small barrier for the transfer of protons from the water molecules to the surface. Ab initio studies on the transfer of proton in water are discussed in more detail by Tuckerman,[46] Scheiner,[47] and by Komatsuzaki and Ohmine.[48] Komatsuzaki and Ohmine observe that the barrier for proton migration between water molecules is a function of the O−O distance between the water molecules. At short O−O distances, the proton transfer potential has a single energy minimum. The minimum occurs when the proton is exactly midway between the two solvating water molecules. At O−O distances which are greater than 2.4 Å, the potential energy surface is reported to have a double well character. The two minima correspond to the configurations in which the central proton is closer to one of the two solvating water molecules. The transfer of proton between the two water molecules is reported to be an activated process when the O−O distance between the water molecules is greater than 2.4 Å. We observe a longer O−O distance between the water molecules (2.45 Å to 2.62 Å), suggesting that there is a barrier for the transfer of proton between water molecules in our system.

The hydrogen bonds between the solvating water molecules and the adsorbed acetate species were observed to weaken the interaction of the acetate intermediate with the metal surface. The Pd−O distances were elongated to 2.24 and 2.17 Å. These distances are longer than those observed when acetate was adsorbed in the vapor phase where the Pd−O distances were 2.11 and 2.13 Å. The two Pd−O bonds are not identical when acetate is surrounded by water molecules. This is because the environment of water molecules in the vicinity of the two oxygen atoms is not symmetric. Even when we started with nearly symmetric structures, geometry optimizations lead to the structure shown here in Figure 10.

A Mulliken charge analysis was performed to provide an estimate of the electron sharing between the products formed on the deprotonation of acetic acid over Pd(111). The acetate species formed by the deprotonation of acetic acid over Pd(111) in the presence of solvating water molecules was found to have an excess negative charge of 0.55 units as compared to the acetate species formed by the dissociation of acetic acid over Pd(111) in the vapor phase. In contrast, the atomic hydrogen that is formed by the deprotonation of acetic acid over Pd(111) in the presence of solvent molecules has a net positive charge of 0.26 units as compared to the hydrogen intermediate formed

by the dissociation of acetic acid in the vapor phase. This suggests that the dissociation of acetic acid over Pd(111) is more heterolytic in the presence of solvent molecules than in the vapor phase. The products formed on the dissociation of acetic acid over Pd(111) have free radical characteristics in the vapor phase and more ionic characteristics in the presence of solvent.

The acetate species that forms as a result of the dissociation is stabilized by the water molecules that are hydrogen-bonded to it as well as by the metal surface. The proton that forms resides in the solvent layer near the surface where it weakly interacts with the negatively charged surface species while being solvated by surrounding water molecules. The dissociation of acetic acid thus results in a *"double layer"* near the metal surface—a layer of acetate anions that is directly adsorbed on the surface followed by a layer of solvated protons. This is analogous to the electrochemical double layer that is known to form at an electrode−electrolyte interface. Due to the finite size of the unit cell in our calculations, it is possible that the formation of the double layer at the Pd(111) surface may have some spurious effect on the computed electronic energy. To fully eliminate the possibility of such an effect, we would need to model the system with a significantly larger unit cell and in turn with a much greater number of water molecules (to maintain a density of about 1 g/cc). Such a calculation is computationally intractable with the present day resources. We have instead, attempted to obtain to a qualitative or semiquantitative estimate of any secondary effects introduced due to the presence of the double layer near the metal surface. We have examined the charge density distribution in two systems—one with a double layer (acetate species adsorbed on Pd(111) and proton in water: Figure 10) and the other without a double layer (water adsorbed on Pd(111): Figure 6). While there are significant differences in the charge density distribution near the metal surface due to the presence of the double layer, we find that the charge density distribution in the two systems is nearly the same beyond 5.5 Å away from the surface. The similarity in the charge distribution away from the surface, despite the presence of a double layer, indicates that any spurious effect on the computed electronic energy of the system due to the presence of the double layer is small.

The energy associated with the heterolytic deprotonation of acetic acid on Pd(111) in the presence of water molecules (eq 5) was found to be +37 kJ/mol. In the gas phase, the heterolytic dissociation of acetic acid into the acetate anion and proton was endothermic by +1483 kJ/mol. The lower endothermicity of dissociation over a metal surface in the presence of solvent is due to the stabilization of the reaction products by the solvating water molecules and by the Pd(111) surface. However, in Section 4.2.2 we showed that the dissociation of acetic acid to acetate and a proton in the presence of water molecules is almost thermoneutral ($\Delta E_{\text{reaction}} = +4$ kJ/mol). In that case, both, the proton and the acetate anion were completely solvated by surrounding water molecules forming strong hydrogen bonds. The deprotonation of acetic acid in water (without metal) is less endothermic (+4 kJ/mol) than deprotonation over Pd(111) in the presence of solvating water molecules (+37 kJ/mol). This suggests that the acetate anion that forms on deprotonation of acetic acid is more stable when it is completely surrounded by water molecules than when it is partly stabilized by Pd(111) and partly by water. Therefore, desorption of the acetate ion from the metal surface into solvating water is likely to be an exothermic process.

To quantify the desorption energy of the acetate ion from Pd(111) surface into the solvating water, we performed periodic slab calculations for a system in which the acetate ion was completely surrounded by water molecules, separating it from direct contact with the Pd(111) surface. Water molecules were used to saturate the metal surface sites where the acetate species once stood. The geometry of the system was optimized to minimize the total SCF electronic energy. The calculations show that the acetate ion is 57 kJ/mol more stable when completely solvated by water molecules than when it is directly adsorbed on the metal surface partly solvated by water molecules.

The structure where acetate is directly adsorbed on the palladium surface and solvated by water molecules is therefore likely a local energy minimum. It is more favorable, in terms of energy, however, for acetate to reside in solution. Since the geometry optimization schemes even at higher time steps did not displace the acetate from the surface to this lower energy state, it is likely that the displacement is an activated process. This suggests that the acetate surface species exist if acetic acid is exposed to the surface before water is. If, on the other hand, water is exposed to the surface first, the acetate ion will more likely prefer to be in the solution rather than in direct contact with the metal surface.

To get an estimate of the acetate−metal interaction energy in the presence of water, we used an approach similar to that used in Section 4.3.2 to determine the water−metal interaction energy in the presence of solvent molecules. The acetate species with all water molecules and the corresponding protons were treated as the "*adsorbate*" for substitution in to RHS of eq 1. The interaction of acetate with Pd(111) surface in the presence of solvent is expected to be weaker than in the "vapor phase" due to partial stabilization of acetate by hydrogen bond formation with the water molecules solvating it. Our calculations estimate that the acetate−Pd(111) interaction in the presence of solvating water molecules is still attractive at −114 kJ/mol. Thus, while the acetate ion is 57 kJ/mol more stable when completely surrounded by water molecules than when bound to Pd(111) surface and partly solvated by water molecules, it has a favorable interaction with the metal surface. There is likely a barrier for the desorption of acetate from Pd(111) surface into water. This can be rationalized if we consider the Pd−O distance as the reaction coordinate for the desorption process. The Pd−O distances for the adsorbed acetate species are shown in Figure 10. The desorption of acetate from Pd(111) surface can be pictured as stretching of the Pd−O bond distance (Figure 11). As the Pd−O distance is increased, the energy of the system is expected to increase since the acetate−metal bonds are broken. At the same time, water molecules are sterically hindered from solvating the desorbing acetate species from below. The energy continues to increase with increasing Pd−O distances up to a certain value. Once the Pd−O distance becomes sufficiently large, water molecules begin to penetrate the acetate adlayer and stabilize the resulting anion from below. The energy will therefore decrease and will continue to do so until the desorbed acetate is completely solvated by water molecules.

Our results are consistent with the general ideas presented by Stuve and co-workers[7] on metal-catalyzed acid dissociation and the effects of water. Although Stuve et al.[7] examined perchloric acid dissociation over Ag(110), which is quite different than acetic acid over palladium, the mechanistic features are quite similar. Perchloric acid adsorbs and dissociates over Ag to form the perchlorate and hydrogen intermediates. Water is subsequently introduced into the UHV chamber whereby it partially solvates the proton as well as the perchlorate intermediate. On the basis of symmetry in the vibrational spectrum the authors conclude that the perchlorate likely loses

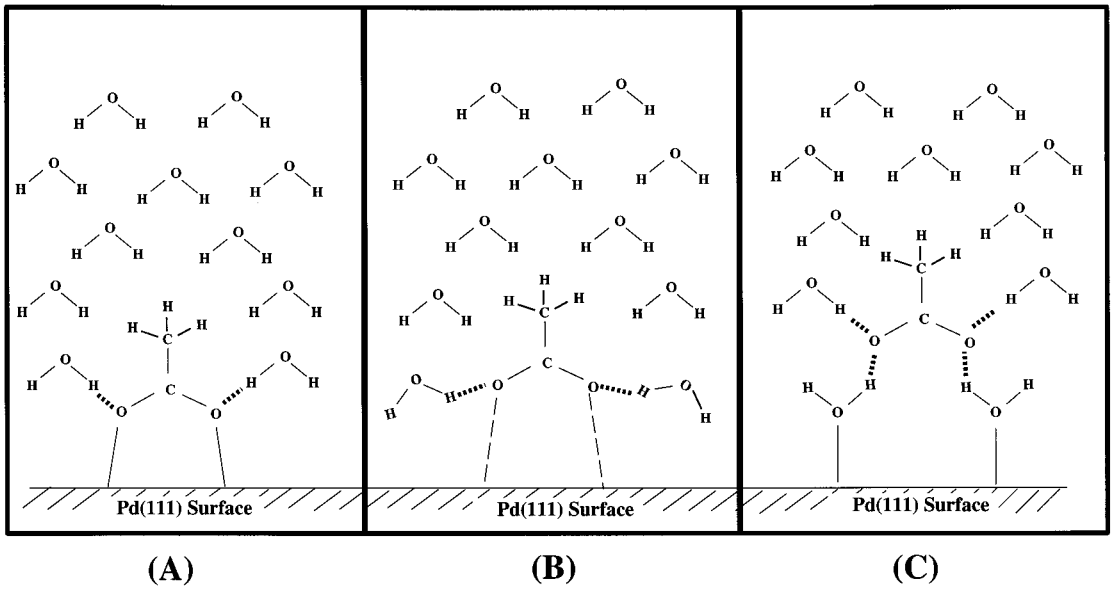

Figure 11. Schematic representation of the desorption of acetate adsorbed on Pd(111) in to bulk water. (A) Acetate adsorbed on Pd(111) and solvated by water molecules from the top; (B) Acetate in the process of desorption. The Pd−O bond distance is stretched as acetate desorbs in to bulk water. Water molecules are sterically hindered from fully solvating the acetate ion; (C) Acetate in bulk water completely solvated by water molecules.

direct contact with the metal surface but remains near the surface. They describe perchlorate as being "nonspecifically adsorbed". Our results differ slightly in that the acetate species that forms remains bound to the surface at 0 K. Although desorption is exothermic, there appears to be an activation barrier that is not overcome at 0 K. As the temperature is increased, higher energy states are populated and the probability that the barrier is overcome increases. We have examined the existence of a barrier for the acetate to desorb from the Pd surface by performing ab initio MD calculations at 300 K and at 1000 K. At 300 K, neither acetic acid nor the acetate species comes off the metal surface. At 1000 K, however, we find that the proton attaches to the adsorbed acetate species to form acetic acid. Acetic acid has a weak interaction with the metal and begins to come off the surface. Water molecules begin to penetrate in to the adlayer. This indicates that there is a barrier for acetate to desorb from the surface that cannot be overcome at 300 K. We have not determined the magnitude of the barrier and will report it in a future communication.

5. Conclusions

We have used first principle periodic density functional theory calculations to examine how solvating water molecules can influence simple bond-breaking reactions on metal surfaces. Specifically, we have examined the deprotonation of acetic acid to acetate and proton on Pd(111).

The heterolytic dissociation of acetic acid into the acetate anion and the corresponding proton is highly endothermic in the gas phase at +1483 kJ/mol. On the other hand, the homolytic dissociation of acetic acid into acetate and hydrogen radicals in the gas phase is endothermic by only +468 kJ/mol and is hence favored over heterolytic dissociation in the gas phase.

The metal surface stabilizes the products formed by the deprotonation of acetic acid. The overall reaction energy for the dissociation of acetic acid over Pd(111) in the vapor phase into acetate and hydrogen surface intermediates is only +28 kJ/mol. A Mulliken charge analysis indicates that the dissociaton of acetic acid over Pd(111) is more homolytic in the vapor phase giving rise to acetate and hydrogen radical like species adsorbed on the surface. However, in the presence of solvating water molecules, the dissociation of acetic acid over Pd(111) is found more heterolytic, producing acetate anion and proton like species.

While the heterolytic dissociation of acetic acid is highly endothermic in the gas phase (+1483 kJ/mol), it was shown to be nearly thermoneutral in the presence of water molecules. Water stabilizes both the acetate ion and the proton formed as a result of the dissociation. The effect of water is more pronounced on the interactions with the proton as compared to the acetate anion on account of higher charge-to-volume ratio of proton. The metal surface also stabilizes the CH_3COO^- like species that form as a result of the dissociation of acetic acid over Pd(111) in the presence of solvent molecules. The stabilization provided by the metal surface, however, is weaker than that by solvent molecules. The overall reaction energy for acetic acid dissociation over Pd(111) in the presence of water molecules was found to be endothermic at +37 kJ/mol. The acetate anion however is 57 kJ/mol more stable if it exists in the water phase rather than on the metal surface.

The presence of solvating water molecules weakens the interaction of the acetate intermediate with the metal surface. In the absence of solvating water molecules, acetate intermediate has a strong attractive interaction at −198 kJ/mol with Pd(111). However, even in the presence of solvating water molecules, the interaction of acetate with the metal surface is attractive at −114 kJ/mol. There is likely to be a barrier for the desorption of acetate anion from the surface into water.

The sequence in which molecules are introduced on a metal surface may be important in determining the surface composition in the presence of solvent molecules. If an aqueous solution containing acetate ions is introduced on a Pd (111) surface, water would preferentially interact with the metal surface. Acetate ions on the other hand would prefer to be in the solvating liquid. However, if acetate ions are introduced first on Pd(111) surface and subsequently water molecules are introduced, acetate would continue to interact with the metal.

Acknowledgment. We thank Professor J. P. O'Connell and Professor R. J. Davis at the University of Virginia for their

valuable discussions. We are also grateful to the National Science Foundation (NSF Career Award CTS-9702762) and the DuPont Chemical Company for providing financial support for the project. Information Technology and Communication (ITC) at the University of Virginia is thankfully acknowledged for providing resources and computer support for this work.

References and Notes

(1) Weaver, M. J. *J. Phys. Chem.* **1996**, *100*, 13079.
(2) Sass, J. K.; Bange, K. *ACS Symp. Ser.* **1988**, *378*, 54.
(3) Bange, K.; Straehler, B.; Sass, J. K.; Parsons, R. *J. Electroanal. Chem.* **1987**, *229*, 87.
(4) Bange, K.; Madey, T. E.; Sass, J. K. *Surf. Sci.* **1985**, *162*, 252.
(5) Stuve, E. M.; Dohl-Oelze, R.; Bange, K.; Sass, J. K. *J. Vac. Sci. Technol. A* **1986**, *4*, 1307.
(6) Dohl-Oelze, R.; Brown, C. C.; Stark, S.; Stuve, E. M. *Surf. Sci.* **1989**, *210*, 339.
(7) Kizhakevariam, N.; Dohl-Oelze, R.; Stuve, E. M. *J. Phys. Chem.* **1990**, *94*, 5934.
(8) Krasnopoler, A.; Stuve, E. M. *J. Vac. Sci. Technol. A* **1995**, *13*, 1681.
(9) van Santen, R. A.; Neurock, M. *Catal. Rev.—Sci. Eng.* **1995**, *37*, 557.
(10) Cramer, C. J.; Truhlar, D. G. Continuum Solvation Models. In *Solvent Effects and Chemical Reactivity*; Tapia, O., Bertran, J., Eds.; Kluwer Academic Publishers: Dordrecht, 1996; Vol. 17, pp 1−80.
(11) Price, D. L.; Halley, J. W. *Chem. Phys.* **1995**, *102*, 6603.
(12) Car, R.; Parrinello, M. *Phys. Rev. Lett.* **1985**, *55*, 2471.
(13) Thiel, P. A.; Madey, T. E. *Surf. Sci. Rep.* **1987**, *7*, 211−385.
(14) Hammer, B.; Hansen, L. B.; Norskov, J. K. *Phys. Rev. B* **1999**, *59*, 7413.
(15) Payne, M. C.; Teter, M. P.; Allan, D. C.; Arias, T. A.; Joannopoulos, J. D. *Rev. Mod. Phys.* **1992**, *64*, 1045−1097.
(16) Gillan, M. J. *J. Phys.: Condens. Matter* **1989**, 1.
(17) Kohn, W.; Sham, L. J. *Phys. Rev.* **1965**, *140*, 1133A.
(18) Chadi, D. J.; Cohen, M. L. *Phys. Rev. B* **1973**, *10*, 4988.
(19) Perdew, J. P.; Chevary, J. A.; Vosko, S. H.; Jackson, K. A.; Pederson, M. R.; Singh, D. J.; Fiolhais, C. *Phys. Rev. B* **1992**, *46*, 6671.
(20) Ceperley, D. M.; Alder, B. J. *Phys. Rev. Lett.* **1980**, *45*, 566.
(21) Perdew, J. P.; Zunger, A. *Phys. Rev. B* **1981**, *23*, 5048.
(22) Ortiz, G.; Ballone, P. *Phys. Rev. B* **1991**, *43*, 6376.
(23) Laasonen, K.; Csajka, F.; Parrinello, M. *Chem. Phys. Lett.* **1992**, *194*, 172.
(24) Troullier, N.; Martins, J. L. *Phys. Rev. B* **1991**, *43*, 1993.
(25) Davis, J. L.; Barteau, M. *Langmuir* **1989**, *5*, 1299.
(26) Pallassana, V.; Neurock, M.; Hansen, L. B.; Hammer, B.; Norskov, J. K. *Phy. Rev. B* **1999**, *60*, 6146.
(27) Jona, F.; Marcus, P. M. In *The Structure of Surfaces II*; Veen, J. F. v. d., Hove, M. A. V., Eds.; Springer: Berlin, 1988; p 90.
(28) Frish, M. J.; Trunks, G. W.; Schlegel, H. B.; Gill, P. M. W.; Johnson, B. G.; Robb, M. A.; Cheeseman, J. R.; Keith, T. A.; Peterson, G. A.; Montgomery, J. A.; Raghavachari, K.; Al-Laham, M. A.; Zakrzewski, V. G.; Ortiz, J. V.; Foresman, J. B.; Ciolowski, J.; Stefanow, B. B.; Nanyaklara, A.; Challacombe, M.; Peng, C. Y.; Ayalo, P. Y.; Chen, W.; Wong, M. W.; Andres, J. L.; Replogle, E. S.; Gomperts, R.; Martin, R. L.; Fox, D. J.; Binkley, J. S.; Defrees, D. J.; Baker, J.; Stewart, J. P.; Head-Gordon, M.; Gonzalez, C.; Pople, J. A.; *Gaussian 94*, Rev B.1 ed.; Gaussian Inc: Pittsburgh, PA, 1995.
(29) Becke, A. D. *J. Chem. Phys.* **1993**, *93*, 5648.
(30) Gonzalez, L.; Mo, O.; Yanez, M. *J. Comput. Chem.* **1997**, *18*, 1124.
(31) Becke, A. D. *J. Chem. Phys.* **1988**, *88*, 1053.
(32) Lee, C.; Yang, W.; Parr, R. G. *Phys. Rev. B* **1988**, *37*, 785.
(33) Heinzinger, K.; Palinkas, G. In *Interactions of Water in Ionic and Nonionic Hydrates*; Kleeberg, H., Ed.; Springer: Heidelberg, 1987; p 1.
(34) Eisenberg, D.; Kauzmann, W. *The Structure and Properties of Water*; Oxford University Press: New York, 1969.
(35) Lias, S. G.; Liebman, J. F.; Levin, R. D. *J. Phys. Chem. Ref. Data* **1984**, *13*, 695.
(36) March, J. *Advanced Organic Chemistry*, 3rd ed.; Wiley: New York, 1985.
(37) Andersson, S.; Nyberg, C.; Tengstal, C. G. *Chem. Phys. Lett.* **1984**, *104*, 305−310.
(38) Stuve, E. M.; Jorgensen, S. W.; Madix, R. J. *Surf. Sci.* **1984**, *146*, 179−198.
(39) Spohr, E. *J. Phys. Chem.* **1989**, *93*, 6171−6180.
(40) Doering, D.; Madey, T. E. *Surf. Sci.* **1982**, *123*, 305.
(41) Bange, K.; Madey, T. E.; Sass, J. K.; Stuve, E. *Surf. Sci.* **1987**, *183*, 334.
(42) Neurock, M.; Kragten, D. D.; van Santen, R. A.; Lerou, J. J. To be submitted.
(43) Paul, J.-F.; Sautet, P. *Surf. Sci.* **1996**, *356*, L403−L409.
(44) Stuve, E.; Kizhakevariam, N. *J. Vac. Sci. Technol. A* **1993**, *11*, 2217−2224.
(45) Tuckerman, M.; Laasonen, K.; Spirk, M. *J. Chem. Phys.* **1995**, *103*, 150.
(46) Tuckerman, M.; Laasonen, K.; Spirk, M.; Parrinello, M. *J. Chem. Phys.* **1995**, *103*, 150.
(47) Scheiner, S. *J. Am. Chem. Soc.* **1981**, *103*, 315.
(48) Komatsuzaki, T.; Ohmine, I. *Chem. Phys.* **1994**, *180*, 239.